



The origin of noise and magnetic hysteresis in permalloy fluxgate sensors

B. B. Narod

The origin of noise and magnetic hysteresis in crystalline permalloy ring-core fluxgate sensors

B. B. Narod^{1,2}

¹Narod Geophysics Ltd., Vancouver, Canada

²Department of Earth, Ocean and Atmospheric Sciences, University of British Columbia, Vancouver, Canada

Received: 19 March 2014 – Accepted: 13 May 2014 – Published: 19 June 2014

Correspondence to: B. B. Narod (bnarod@eos.ubc.ca)

Published by Copernicus Publications on behalf of the European Geosciences Union.

[Title Page](#)

[Abstract](#)

[Introduction](#)

[Conclusions](#)

[References](#)

[Tables](#)

[Figures](#)

[⏪](#)

[⏩](#)

[◀](#)

[▶](#)

[Back](#)

[Close](#)

[Full Screen / Esc](#)

[Printer-friendly Version](#)

[Interactive Discussion](#)



Abstract

6-81.3Mo permalloy, developed in the 1960s for use in high performance ring-core fluxgate sensors, remains the state-of-the-art for permalloy-cored fluxgate magnetometers. The magnetic properties of 6-81.3, namely magnetocrystalline and magnetoelastic anisotropies and saturation induction are all optimum in the Fe–Ni–Mo system.

In such polycrystalline permalloy fluxgate sensors a single phenomenon may cause both fluxgate noise and magnetic hysteresis, explain Barkhausen jumps, remanence and coercivity, and avoid domain denucleation. The phenomenon, domain wall reconnection, is presented as part of a theoretical model. In the unmagnetized state a coarse-grain high-quality permalloy foil ideally forms stripe domains, which present at the free surface as parallel, uniformly spaced domain walls that cross the entire thickness of the foil. Leakage flux “in” and “out” of alternating domains is a requirement of the random orientation, grain-by-grain, of magnetic easy axes’ angles with respect to the foil free surface. Its magnetostatic energy together with domain wall energy determines an energy budget to be minimized. Throughout the magnetization cycle the free surface domain pattern remains essentially unchanged, due to the magnetostatic energy cost such a change would elicit. Thus domain walls are “pinned” to free surfaces.

Driven to saturation, domain walls first bulge then reconnect via Barkhausen jumps to form a new domain configuration this author has called “channel domains”, that are attached to free surfaces. The approach to saturation now continues as reversible channel domain compression. Driving the permalloy deeper into saturation compresses the channel domains to arbitrarily small thickness, but will not cause them to denucleate. Returning from saturation the channel domain structure will survive through zero H , thus explaining remanence. The Barkhausen jumps being irreversible exothermic events are sources of fluxgate noise, powered by the energy available from domain wall reconnection.

The origin of noise and magnetic hysteresis in permalloy fluxgate sensors

B. B. Narod

[Title Page](#)

[Abstract](#)

[Introduction](#)

[Conclusions](#)

[References](#)

[Tables](#)

[Figures](#)

[⏪](#)

[⏩](#)

[◀](#)

[▶](#)

[Back](#)

[Close](#)

[Full Screen / Esc](#)

[Printer-friendly Version](#)

[Interactive Discussion](#)



The origin of noise and magnetic hysteresis in permalloy fluxgate sensors

B. B. Narod

[Title Page](#)

[Abstract](#)

[Introduction](#)

[Conclusions](#)

[References](#)

[Tables](#)

[Figures](#)

[⏪](#)

[⏩](#)

[◀](#)

[▶](#)

[Back](#)

[Close](#)

[Full Screen / Esc](#)

[Printer-friendly Version](#)

[Interactive Discussion](#)



A simplified domain energy model can then provide a predictive relation between ring core magnetic properties and fluxgate sensor noise power. Four properties are predicted to affect noise power, two of which, are well known: saturation total magnetic flux density and magnetic anisotropy. The two additional properties are easy axes alignment and foil thickness. Flux density and magnetic anisotropy are primary magnetic properties determined by an alloy's chemistry and crystalline lattice properties. Easy axes alignment and foil thickness are secondary, geometrical properties related to an alloy's polycrystalline fabric and manufacture. Improvements to fluxgate noise performance can in principle be achieved by optimizing any of these four properties in such a way as to minimize magnetostatic energy.

Fluxgate signal power is proportional to $B-H$ loop curvature (d^2B/dH^2). The degree to which Barkhausen jumps coincide with loop curvature is a measure of noise that accompanies fluxgate signal. $B-H$ loops with significant curvature beyond the open hysteresis loop may be used to advantage to acquire fluxgate signal with reduced noise.

1 Introduction

The 1979 launch of the NASA spacecraft MAGSAT marked a milestone in the development of magnetometry. In particular it terminated an effort by a group at Naval Ordnance Laboratory, led by Daniel Israel Gordon, to create a low-noise magnetic alloy now referred to as 6-81.3Mo permalloy, “6-81” (Gordon et al., 1968). Answering the question of why 6-81.3Mo permalloy became the de facto standard for low noise ring core fluxgates is the first motivation for this paper.

I begin with an examination of data that relate fluxgate noise to various physical parameters and provide evidence that the geometric configurations of a fluxgate's magnetic material are significantly more important than Gordon's investigators may have thought. As surface area, either free surface or intergrain, of the magnetic material increases, so does the fluxgate noise power. This suggests there is a causal link

The origin of noise and magnetic hysteresis in permalloy fluxgate sensors

B. B. Narod

[Title Page](#)

[Abstract](#)

[Introduction](#)

[Conclusions](#)

[References](#)

[Tables](#)

[Figures](#)

[⏪](#)

[⏩](#)

[◀](#)

[▶](#)

[Back](#)

[Close](#)

[Full Screen / Esc](#)

[Printer-friendly Version](#)

[Interactive Discussion](#)

between fluxgate noise and magnetostatic energy by way of domain wall energy, and that all are fundamentally dependent on the properties magnetic moment and anisotropy.

Amos et al. (2008) using magnetic force microscopy (MFM) have shown that sputtered permalloy films assume configurations called “stripe domains.” Thus it should be beneficial to examine the causes of stripe domains. Since fluxgate sensor function requires periodic core saturation in order to generate a signal, it is also beneficial to study the evolution of stripe domains throughout the magnetization cycle.

Recently Coisson et al. (2009) also using MFM, have determined the surface expression of stripe domains in sputtered films throughout the magnetization cycle, confirming constraints on magnetostatic energy which can be derived from simple principles. I propose that on approach to saturation each stripe domain undergoes a well-defined, exothermic and irreversible transition to a saturated state, with domain wall loss supplying the energy. It further follows that these transitions could be used to explain many aspects of irreversible and reversible magnetization processes in magnetically soft materials, in particular DC coercivity, remanence and hysteresis.

Fluxgate noise and DC hysteresis are thus arguably two facets of the same phenomenon, and that fluxgate sensor noise is causally tied to domain wall energy by a simple relationship: fluxgate noise is proportional to available domain wall energy, which itself is a function of domain size and domain wall energy density.

Magnetocrystalline anisotropy complicates the story: in any polycrystalline permalloy each crystal assumes an easy axis from a distribution, an axis that in general will not lie parallel to the magnetizing field, nor to the free surface. This affects domain size and local magnetization processes. Saturation transitions in one crystal will not in general coincide with those in any other crystal. Fluxgate noise and a ferromagnet’s path to saturation will be an aggregate of all the individual crystals’ processes. But the basic phenomena can be understood by examining processes in a single, ideal crystal.

3 Geometrical evidence towards a theory of noise

Two more observations provide evidence for the last clues needed for a theory of noise. Figure 2 plots dB/dt vs. t , an analog for DC differential permeability vs. H for five ring cores, two of material 6-81 and three of 4-79 permalloy, each annotated with its noise power. Lower noise power correlates with higher peak dB/dt . Similarly amorphous alloys treated at temperatures up to 350°C will develop large magnetic domains (Shishido et al., 1985), and treating such alloys to about 300°C will significantly reduce their noise power (Narod et al., 1985). The 4-79 rings exhibit both higher noise power and higher coercivity (peaks are to the right of the 6-81 curves). This is likely a grain size effect (Pfeifer and Radaloff, 1980).

An hypothesis follows: (1) larger domain sizes lead to both lower noise and to higher differential permeability, (2) smaller grain size leads to higher domain wall energy, noise power and coercivity. It then follows that total domain wall area is also related to fluxgate sensor noise.

A last clue comes from my examination of noise in a large collection of Infnetics “6-81” ring cores. This included 195 $12\ \mu\text{m}$ rings with 7 layers each, and 75 $3\ \mu\text{m}$ rings with 28 layers. Otherwise these rings are similar. Figure 3 plots the noise PDFs for this collection, with $3\ \mu\text{m}$ rings’ data in white, and $12\ \mu\text{m}$ data in black. Counts have been scaled to match. These data show clearly that the $3\ \mu\text{m}$ rings are typically 12 dB noisier than the $12\ \mu\text{m}$ rings. Equally, the $3\ \mu\text{m}$ rings have four times the free surface area, the same ratio. With such a large number of specimens, from a large number of independent processing batches, this statistic is robust and cannot have happened by chance. Clearly the geometry of the fluxgate core material matters, and any theory of fluxgate noise must be able to take this into account.

The origin of noise and magnetic hysteresis in permalloy fluxgate sensors

B. B. Narod

[Title Page](#)

[Abstract](#)

[Introduction](#)

[Conclusions](#)

[References](#)

[Tables](#)

[Figures](#)

[⏪](#)

[⏩](#)

[◀](#)

[▶](#)

[Back](#)

[Close](#)

[Full Screen / Esc](#)

[Printer-friendly Version](#)

[Interactive Discussion](#)



Typically D and t are of the same magnitude with $D < t$ except for very thin films. Figure 6 extends the concepts of Fig. 5 to examine a small portion of a core, within a single crystal, one that occupies the entire thickness of the core foil material.

Areal domain wall energy density can be approximated as

$$E_d = 2\pi\sqrt{\frac{JS^2K}{a}} \propto 2\pi\sqrt{\frac{B_s^2K}{a}}. \quad (5)$$

K is a parameter representing all of magnetic anisotropy, J is the exchange integral, S is the magnitude of atomic spin, and a is the lattice constant (Chikazumi, 1997). B_s^2 is proportional to JS^2 given that J is proportional to Curie temperature T_c (Weiss, 1948), T_c is proportional to magnetic moment-squared M^2 (Chikazumi, 1997, Eq. 6.8), and B_s correlates strongly with M (Fig. 14). The substitution with B_s requires the assumption that FCC lattice parameters, spin magnitude and molecular field coefficient vary little or not at all compared with variation of B_s over the range of permalloy compositions.

Magnetic anisotropy for cubic alloys has higher order terms. Reducing anisotropy to a single parameter however does not significantly impact our aim which is to calculate total domain wall energy and total magnetostatic energy, and minimize their sum to determine domain width. Magnetostatic energy is required on the free surface of a permalloy foil as all crystalline permalloys have nonzero anisotropy and an easy axis that dips across the free surface at some angle α . Flux density across the free surface is thus about αB_s , where a small angle is assumed for α . Figure 6 indicates the associated flux paths as curved arrows originating from one domain and returning to an adjacent domain.

For soft magnetic materials the calculation is slightly more complicated, with three energies to equilibrate: domain wall energy E_d , magnetostatic energy E_s and magnetic anisotropy energy E_c . Assuming uniform spin rotation and neglecting free surface

The origin of noise and magnetic hysteresis in permalloy fluxgate sensors

B. B. Narod

[Title Page](#)

[Abstract](#)

[Introduction](#)

[Conclusions](#)

[References](#)

[Tables](#)

[Figures](#)

[⏪](#)

[⏩](#)

[◀](#)

[▶](#)

[Back](#)

[Close](#)

[Full Screen / Esc](#)

[Printer-friendly Version](#)

[Interactive Discussion](#)



depolarization these energies (per unit volume), are

$$E_d \propto 2\pi \frac{\sqrt{B_s^2 K/a}}{D}; \quad E_s = (\beta B_s)^2 \frac{D}{t\mu_0} \quad (6)$$

$$E_c = (\alpha - \beta)^2 K$$

where β is the actual magnetization dip angle with respect to the free surface. Similar to the approach taken in Butta and Ripka (2008), the total energy is minimized when E_d equals E_s and when the dip angle

$$\beta = \alpha \frac{1}{1 + \frac{D}{t} \frac{B_s^2}{K\mu_0}}. \quad (7)$$

For the thick foils used in typical ringcores the two angles become equal, and D is proportional to $t^{1/2}$. In this case E_c vanishes and the equilibrium approaches that derived by Kittel (1949). In Amos et al. (2008) for films below $1 \mu\text{m}$, a square-root relation between D and t held, implying a value for K such that the angle $\beta = \alpha$.

The above calculation is for uniformly spaced, flat domain walls. When an external field is applied in a direction along the length of the domains the initial response is to move the domain walls such that net magnetization adapts to the applied field. However the magnetostatic energy constraint at the free surface requires that the domains' surface expression remains essentially unchanged at a uniform distribution, i.e., 50–50% magnetic flux in and out. (Any deviation from 50–50% would require a very large energy expense. Magnetostatic energy E_s could no longer be localized near the free surface.) It follows that for a small field the domain walls must adapt as shown in Fig. 7. E_s increases with negligible surface change while domain wall energy increases due to the longer arc length of the domain wall across the foil thickness.

Increasing the applied field further expands the domain wall (Fig. 8a). Eventually a field value is reached where adjacent domain walls make contact (Fig. 8b) at which

The origin of noise and magnetic hysteresis in permalloy fluxgate sensors

B. B. Narod

[Title Page](#)

[Abstract](#)

[Introduction](#)

[Conclusions](#)

[References](#)

[Tables](#)

[Figures](#)

[⏪](#)

[▶⏩](#)

[◀](#)

[▶](#)

[Back](#)

[Close](#)

[Full Screen / Esc](#)

[Printer-friendly Version](#)

[Interactive Discussion](#)



The origin of noise and magnetic hysteresis in permalloy fluxgate sensors

B. B. Narod

[Title Page](#)

[Abstract](#)

[Introduction](#)

[Conclusions](#)

[References](#)

[Tables](#)

[Figures](#)

[⏪](#)

[⏩](#)

[◀](#)

[▶](#)

[Back](#)

[Close](#)

[Full Screen / Esc](#)

[Printer-friendly Version](#)

[Interactive Discussion](#)

point a domain wall reconnection occurs (Fig. 8c), forming a new configuration in which a pair of arched domains is left to satisfy the magnetostatic energy boundary condition. Domain wall area is reduced by this reconnection. The event is irreversible and exothermic, with excess energy dissipated thermally as eddy currents. Such an irreversible event must have random activation energy and thus must be a source of noise. One can identify such a reconnection with a Barkhausen jump. Further field increases serve to reversibly compress these new domains (Fig. 8d), which I shall call “channel domains” to distinguish them from the original stripe domains. However the free surface expression of the channel domains remains, and the domains themselves cannot denucleate.

In Coisson et al. (2009) their Fig. 4 (here as Fig. 9) provides evidence for the formation of channel domains. MFM images of the domains’ surface expressions for the two polarizations of a saturated specimen are practically indistinguishable, and substantiate the strength of the magnetostatic energy boundary condition. (To be clear, in crystalline alloys the stripe domains would form due to magneto-crystalline anisotropy and not spin reorientation (Coisson et al., 2009; Sharma et al., 2006). Their test material was an iron-metalloid sputtered film, but arguably the magnetostatic energy constraints should be similar.)

The saturated state thus is one of channel domains, which being shallow and bounded by a free surface are relatively difficult to compress (low permeability). The demagnetized state is dominated by stripe domains. Walls are relatively easy to move, and reconnections present as large values of differential permeability (Barkhausen jumps). In general the distribution of individual crystals’ easy axes will be random. This results in a range of H values for which reconnections will occur in a bulk specimen, and any attempt to estimate differential permeability will need to take this into account. The return from saturation starts by expanding the channel domains, similar to inflating a bubble (Fig. 10). Channel domains self-align across the thickness of the foil, due to the transverse magnetic moments of the channels having opposing magnetic charges, attracting each other by a mechanism broadly similar to one found

The origin of noise and magnetic hysteresis in permalloy fluxgate sensors

B. B. Narod

[Title Page](#)

[Abstract](#)

[Introduction](#)

[Conclusions](#)

[References](#)

[Tables](#)

[Figures](#)

[⏪](#)

[⏩](#)

[◀](#)

[▶](#)

[Back](#)

[Close](#)

[Full Screen / Esc](#)

[Printer-friendly Version](#)

[Interactive Discussion](#)



by O'Brien et al. (2009) for transverse domains in permalloy nanowires. Initially the domain walls extend slowly, requiring a lot of variation of H for relatively little gain in net B , thus the slowly changing but accelerating tops of the hysteresis curve. The channel domains begin to expand adding domain wall area and requiring energy to do that – the energy of hysteresis. Eventually the channels themselves reconnect via a second, smaller Barkhausen jump to again form stripe domains and the process repeats, now in the opposing polarity. For stripe domains reconnecting into channels a lot of domain wall energy is released. For channel domains converting to stripes the amount of energy available is much less clear. The field value at which this occurs is likely closely related to what we can observe as coercivity H_c .

Using Eqs. (6) and (7), solving for and eliminating D , one finds that for a demagnetized stripe domain system, domain wall energy per unit volume is proportional to

$$E_d \propto t^{-1/2} \times \alpha \times B_s^{3/2} \times K^{1/4}. \quad (8)$$

A hypothesis that fluxgate noise power is proportional to E_d can now predict all of the principal observations. Noise power increases as foil thickness decreases, or as B_s or anisotropy increase. Equation (8) also predicts that easy axis dip angle is an important element in creating noise, with small dip angles to be desired, and may explain some of the results of Fig. 2, whereby lower dip angles lead to reduced magnetostatic energy. Stripe domain reconnection energy should not vary with the rate dH_d/dt . Thus energy released per cycle, and thus noise energy per cycle is independent of a fluxgate's drive frequency, consistent with this author's experience.

6 Putting it to the test

Two of the four parameters given in Eq. (8), B_s and anisotropy, are well known to be involved in producing fluxgate noise. With Marc Lessard and others at University of New

reconnections from stripes to channels. All the energy released by these events couples back into the H_d drive circuit and no noise energy gets into the sensor winding.

From B to D curvature is larger, reaching a maximum at point C. Over this interval energy is transferred to the sensor winding. Since in this range changes in B are still dominated by stripe to channel reconnections, it is here that fluxgate noise power is generated, ending at D. From D to E changes in B can result from domain wall movement in the form of channel domain compression. Our new ring cores exhibit significant curvature in this range, resulting in its round $B-H$ curve. This curvature generates additional sensor energy, and since the process of channel domain compression is nominally a reversible process this additional sensor energy comes with little noise energy when compared with interval B-D.

The inset to Fig. 11c is a detail showing in the 100 μm data a well-defined transition from irreversible behaviour to reversible behaviour, a transition not noticeable in the return path. Such a sharp transition requires a magnetization process that can support such transitions and that provides for an entirely reversible process above the transition point. Conventional thinking calls for reversible rotation to explain much of the approach to saturation from D to E (Chikazumi, 1997, Fig. 18.26), the realignment *en masse* of individual electronic spins. Being a body force such realignment should not depend on geometry, particularly material thickness. Comparing the 12 and 100 μm curves in Fig. 11 dispels this possibility. The hysteresis loop closure points marked "+" indicate where reversibility begins. Given that all other variables have been constrained one would expect the two $B-H$ curves to the right of these points to coincide, and clearly this is not the case. Reversible rotation on its own would require average easy axis misalignment of 45% to explain the 30% reversible approach to saturation in Fig. 11c. This is unlikely, implying a need for reversible domain wall motion.

From E to D and part way to point F, an interval of channel domain expansion, energy may be recaptured from the sensor winding. From D to F the $B-H$ curve is dominated by small Barkhausen jumps which can be identified with channel-to-stripe reconnections (Chikazumi, 1997, Fig. 18.43). From point F to point G the $B-H$ curve

The origin of noise and magnetic hysteresis in permalloy fluxgate sensors

B. B. Narod

[Title Page](#)

[Abstract](#)

[Introduction](#)

[Conclusions](#)

[References](#)

[Tables](#)

[Figures](#)

[◀](#)

[▶](#)

[◀](#)

[▶](#)

[Back](#)

[Close](#)

[Full Screen / Esc](#)

[Printer-friendly Version](#)

[Interactive Discussion](#)



The origin of noise and magnetic hysteresis in permalloy fluxgate sensors

B. B. Narod

[Title Page](#)

[Abstract](#)

[Introduction](#)

[Conclusions](#)

[References](#)

[Tables](#)

[Figures](#)

[⏪](#)

[⏩](#)

[◀](#)

[▶](#)

[Back](#)

[Close](#)

[Full Screen / Esc](#)

[Printer-friendly Version](#)

[Interactive Discussion](#)



surfaces so too should they form at intergrain boundaries. This source of magnetostatic energy must give rise to additional domain walls. Energy needed to reconnect the intergrain channel domains back to stripes will manifest as an increase in hysteresis loss, and relates to the known inverse relation between grain size and coercivity (Couderchon et al., 1989; Herzer, 1990; Pfeifer and Radloff, 1980). Speculating further, if larger grains lead to longer magnetic domains then considered as a solenoid each domain's local field near its surface would decrease with increasing grain size. This implies a given amount of domain wall displacement requires less drive field to achieve equilibrium, and by extension that domain wall reconnections require less field (Fig. 13). These are respectively interpretable as higher initial permeability and lower coercivity, both known to correlate with lower fluxgate noise (Nielsen et al., 2010).

Our 6-81 material, with over twice the coercivity of the Infinitics material, must have significantly more magnetostatic energy. An electron micrograph (Kuyucak, 1996) of an Infinitics 3 μm ring core showed grains with 10 μm average size – much larger than the foil thickness. For the 3 μm rings free surface magnetostatic energy must dominate its energy budget.

7 Additional considerations

Equation (8) can be used to guide choices in magnetic materials and in ring core geometry. Regarding the choice of material, clearly “6-81” has very desirable properties. To improve further we need to look for lower B_s materials while simultaneously maintaining low anisotropy. Within the quaternary system Fe–Ni–Mo–Cu it is possible to estimate B_s by calculating an alloy's average atomic moment: $B_m = \text{at\% Fe} \cdot 2.8 + \text{at\% Ni} \cdot 0.6 - \text{at\% Mo} \cdot 4.6 - \text{at\% Cu} \cdot 0.4$, and correlating that with B_s . Figure 14 summarizes such data. The open square marked “3” locates “6-81”. The circle marked “6” locates Neumann's “1040” alloy, which is a possible contender for an improved fluxgate core material due to its lower B_s .

The origin of noise and magnetic hysteresis in permalloy fluxgate sensors

B. B. Narod

[Title Page](#)

[Abstract](#)

[Introduction](#)

[Conclusions](#)

[References](#)

[Tables](#)

[Figures](#)

[⏪](#)

[⏩](#)

[◀](#)

[▶](#)

[Back](#)

[Close](#)

[Full Screen / Esc](#)

[Printer-friendly Version](#)

[Interactive Discussion](#)



Reducing magnetostatic energy by reducing free surface area is an obvious method to reduce domain wall energy. The use of thicker foils or even wires are two such means, both relatively easily achieved. Reducing intergrain surface area is also a means to reduce magnetostatic energy, to be achieved by the application of specific heat treatments tailored to growing large crystals. Ideally a typical grain would be the full thickness of the foil or wire and its diameter much larger. Cold forming to control for easy axis direction might also be an approach to further reduce domain wall energy.

8 Conclusion

I have presented evidence by both data and theory that noise power in the parallel-gated fluxgate has its origin in domain wall energy that transforms irreversibly and exothermically to eddy current energy when domain walls reconnect, identifiable with Barkhausen jumps. Domain wall energy available for noise generation is maintained in a balance with magnetostatic energy, which in thin foils is dominated by the anisotropy-driven surface magnetostatic energies. Reducing surface area thus reduces noise energy.

E_d , and thus fluxgate noise is reduced by treating the permalloy for low anisotropy. However the biggest influence on E_d is the saturation total magnetic flux density B_s . Reducing B_s simultaneously reduces all energies. Its only limitation is a need to concurrently reduce Curie temperature.

These argue for the existence of a previously unidentified magnetic domain state I have called “channel domains.” A channel domain hypothesis can be expressed as follows: in the presence of no external field an individual crystal of a soft magnetic metal can assume one of three magnetized states. One state, in the form of stripe domains, has zero net magnetization. The second and third states, in the form of channel domains of different polarizations, have non-zero net magnetization. A stripe domain or a channel domain state can convert to the other by domain wall expansion and irreversible reconnection, respectively a large or small Barkhausen jump. The

The origin of noise and magnetic hysteresis in permalloy fluxgate sensors

B. B. Narod

[Title Page](#)

[Abstract](#)

[Introduction](#)

[Conclusions](#)

[References](#)

[Tables](#)

[Figures](#)

[⏪](#)

[⏩](#)

[◀](#)

[▶](#)

[Back](#)

[Close](#)

[Full Screen / Esc](#)

[Printer-friendly Version](#)

[Interactive Discussion](#)



three states, stripe domains or channel domains, can satisfy nearly identical surface boundary conditions. The combination of crystals in a stripe domain state and those in a channel domain state is arbitrary and will depend on the history of external fields. DC hysteresis results from the cycling between stripe and channel domain states, via Barkhausen jumps.

Much work remains. Specimens need to be created which have much larger grain sizes than in existing materials. This will require heat treatments at higher temperatures and of longer durations than normally used for permalloys. Domain imaging of large grain, low anisotropy crystalline permalloys throughout a magnetization cycle should provide further testing of the the hypothesis. Combining domain imaging with the manipulation of final heat treatments could determine the relations between anisotropy, domain sizes and fluxgate noise. Fabric analysis could provide data regarding easy axes alignments. Micromagnetic numerical simulations of stripe domain systems with pinned free surface expressions could lead to understanding the energetics of domain wall reconnections.

In the future careful examinations of reconnection processes might be able to draw connections between micromagnetic mechanisms and large scale, phenomenological models (Bertotti, 2008). The existence of channel domain states may go a long way to understanding many phenomena in magnetically soft polycrystalline metals including: remanence, DC coercivity, asymmetry in the $B-H$ loop; solving the “domain nucleation problem”; an irreversible, exothermic process that produces both fluxgate and Barkhausen noise.

Acknowledgements. I thank J. R. Bennest, G. Cross, and S. Allegretto, who assisted on this manuscript. The Geological Survey of Canada made available the collection of “6-81” ring-cores. I thank S. Kuyucak of CANMET, P. Dosanjh at UBC, M. Lessard and the others at UNH, and L. Jewitt, Laura K Jewitt Design Gallery, for their efforts in creating the new 6-81 ring cores.

The origin of noise and magnetic hysteresis in permalloy fluxgate sensors

B. B. Narod

[Title Page](#)

[Abstract](#)

[Introduction](#)

[Conclusions](#)

[References](#)

[Tables](#)

[Figures](#)

[⏪](#)

[⏩](#)

[◀](#)

[▶](#)

[Back](#)

[Close](#)

[Full Screen / Esc](#)

[Printer-friendly Version](#)

[Interactive Discussion](#)



- O'Brien, L., Petit, D., Zeng, H. T., Lewis, E. R., Sampaio, J., Jausovec, A. V., Read, D. E., and Cowburn, R. P.: Near-field interaction between domain walls in adjacent permalloy nanowires, *Phys. Rev. Lett.*, 103, 077206, doi:10.1103/PhysRevLett.103.077206, 2009.
- Pfeifer, F.: Zum Verständnis der magnetischen Eigenschaften technischer Permalloylegierungen, *Z. Metallkd.*, 57, 295–300, 1966 (in German).
- Pfeifer, F. and Boll, R.: New soft magnetic alloys for applications in modern electrotechnics and electronics, *IEEE T. Magn.*, 5, 365–370, 1969.
- Pfeifer, F. and Radaloff, C.: Soft magnetic Ni–Fe and Co–Fe alloys – some physical and metallurgical aspects, *J. Magn. Magn. Mater.*, 19, 190–207, 1980.
- Primdahl, F.: The fluxgate mechanism, Part I: The gating curves of parallel and orthogonal fluxgates, *IEEE T. Magn.*, 6, 376–383, 1970.
- Primdahl, F., Brauer, P., Merayo, J. M. G., and Nielsen, O. V.: The fluxgate ring-core internal field, *Measurement Sci. Technol.*, 13, 1248–1258, 2002.
- Sharma, P., Kimura, H., Inoue, A., Arenholz, E., and Guo, J.-H.: Temperature and thickness driven spin-reorientation transition in amorphous Co–Fe–Ta–B thin films, *Phys. Rev. B*, 73, 052401, doi:10.1103/PhysRevB.73.052401, 2006.
- Shirae, K.: Noise in amorphous magnetic materials, *IEEE T. Magn.*, 20, 1299–1301, 1984.
- Shishido, H., Kann, T., and Ito, Y.: The magnetic domain and properties of amorphous ribbons, *IEEE T. Magn.*, 21, 49–52, 1985.
- von Auwers, O. and Neumann, H.: Über Eisen-Nickel-Kupfer-Legierungen hoher Anfangspermeabilität, *Wissenschaftliche Veröffentlichungen aus den Siemens-Werken*, Berlin, Germany, 14, 92–108, 1935 (in German).
- Weiss, P. R.: The Application of the Bethe-Peierls Method to Ferromagnetism, *Phys. Rev.*, 74, 1493–1504, 1948.

The origin of noise and magnetic hysteresis in permalloy fluxgate sensors

B. B. Narod

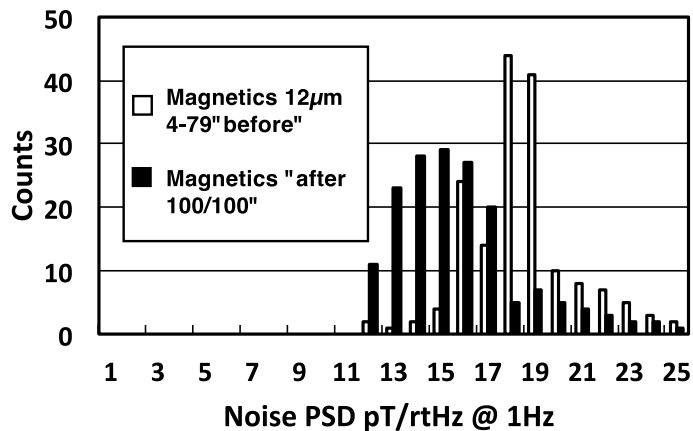


Figure 1. Histograms of noise power for 4-79 permalloy ring-cores.

[Title Page](#)

[Abstract](#)

[Introduction](#)

[Conclusions](#)

[References](#)

[Tables](#)

[Figures](#)

[◀](#)

[▶](#)

[◀](#)

[▶](#)

[Back](#)

[Close](#)

[Full Screen / Esc](#)

[Printer-friendly Version](#)

[Interactive Discussion](#)

The origin of noise and magnetic hysteresis in permalloy fluxgate sensors

B. B. Narod

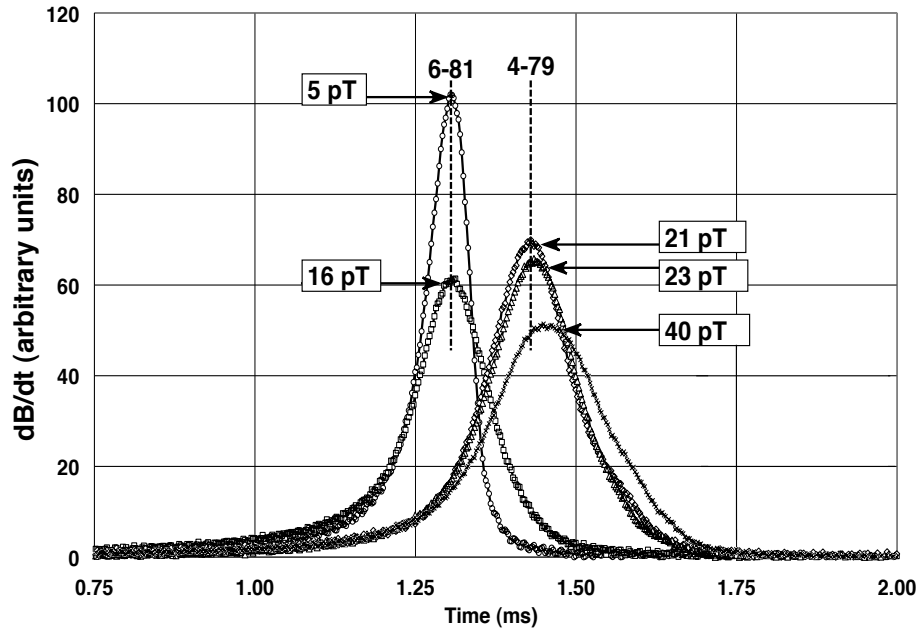


Figure 2. dB/dt plots for 6-81 and 4-79 ring-cores. Noise values are in pT rtHz^{-1} at 1 Hz, for this insert and all other data in this paper.

[Title Page](#)

[Abstract](#)

[Introduction](#)

[Conclusions](#)

[References](#)

[Tables](#)

[Figures](#)

[⏪](#)

[⏩](#)

[◀](#)

[▶](#)

[Back](#)

[Close](#)

[Full Screen / Esc](#)

[Printer-friendly Version](#)

[Interactive Discussion](#)



The origin of noise and magnetic hysteresis in permalloy fluxgate sensors

B. B. Narod

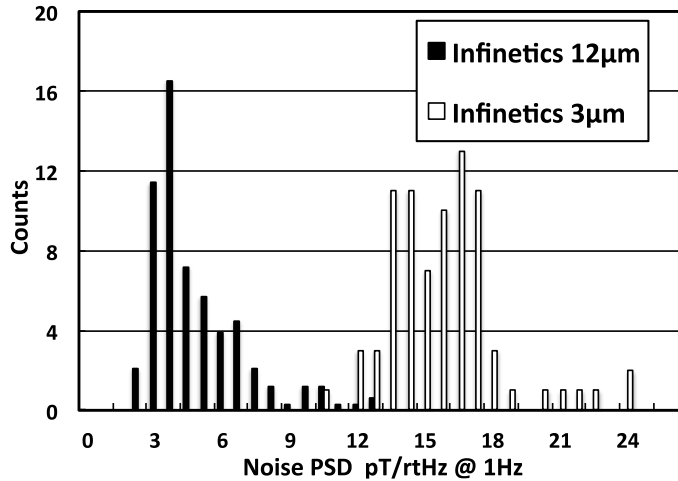


Figure 3. Histograms of noise power for 6-81 permalloy ring-cores.

Title Page	
Abstract	Introduction
Conclusions	References
Tables	Figures
⏪	⏩
◀	▶
Back	Close
Full Screen / Esc	
Printer-friendly Version	
Interactive Discussion	



The origin of noise and magnetic hysteresis in permalloy fluxgate sensors

B. B. Narod

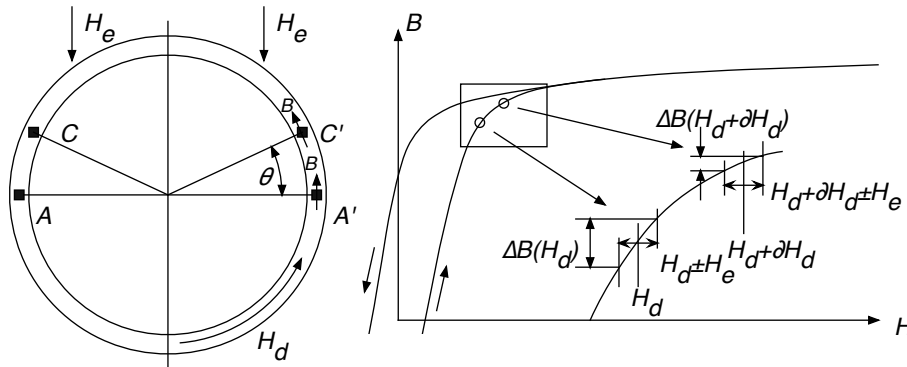


Figure 4. Ring core schematic and $B-H$ loop detail.

[Title Page](#)

[Abstract](#)

[Introduction](#)

[Conclusions](#)

[References](#)

[Tables](#)

[Figures](#)

[◀](#)

[▶](#)

[◀](#)

[▶](#)

[Back](#)

[Close](#)

[Full Screen / Esc](#)

[Printer-friendly Version](#)

[Interactive Discussion](#)



The origin of noise and magnetic hysteresis in permalloy fluxgate sensors

B. B. Narod

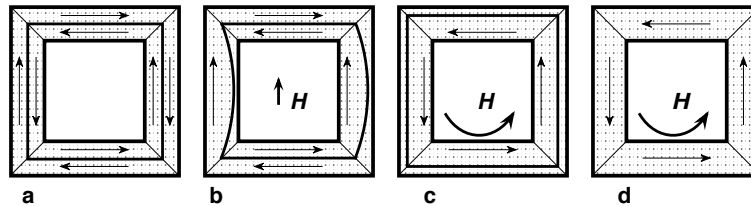


Figure 5. Ring-core domains: responses to external or excitation fields.

[Title Page](#)

[Abstract](#)

[Introduction](#)

[Conclusions](#)

[References](#)

[Tables](#)

[Figures](#)



[Back](#)

[Close](#)

[Full Screen / Esc](#)

[Printer-friendly Version](#)

[Interactive Discussion](#)

The origin of noise and magnetic hysteresis in permalloy fluxgate sensors

B. B. Narod

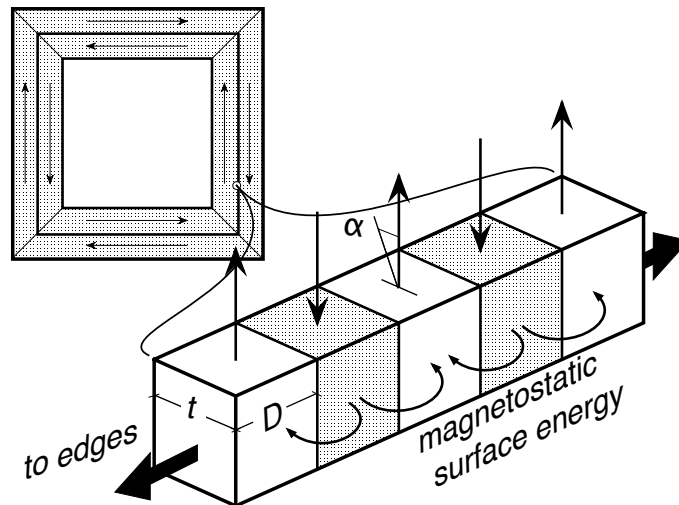


Figure 6. Detail of stripe domains in a demagnetized core. Thin arrows depict magnetic flux, the larger, vertical arrows indicating the dominant flux internal to the core, and the looped arrows depicting the smaller but significant flux crossing the free surface.

[Title Page](#)

[Abstract](#)

[Introduction](#)

[Conclusions](#)

[References](#)

[Tables](#)

[Figures](#)

⏪

⏩

◀

▶

[Back](#)

[Close](#)

[Full Screen / Esc](#)

[Printer-friendly Version](#)

[Interactive Discussion](#)

GID

4, 319–352, 2014

The origin of noise and magnetic hysteresis in permalloy fluxgate sensors

B. B. Narod

[Title Page](#)

[Abstract](#)

[Introduction](#)

[Conclusions](#)

[References](#)

[Tables](#)

[Figures](#)

[⏪](#)

[⏩](#)

[◀](#)

[▶](#)

[Back](#)

[Close](#)

[Full Screen / Esc](#)

[Printer-friendly Version](#)

[Interactive Discussion](#)

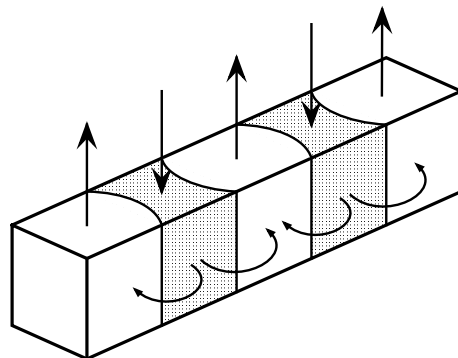


Figure 7. Domain wall motion for initial permeability.

The origin of noise and magnetic hysteresis in permalloy fluxgate sensors

B. B. Narod

[Title Page](#)

[Abstract](#)

[Introduction](#)

[Conclusions](#)

[References](#)

[Tables](#)

[Figures](#)

[◀](#)

[▶](#)

[◀](#)

[▶](#)

[Back](#)

[Close](#)

[Full Screen / Esc](#)

[Printer-friendly Version](#)

[Interactive Discussion](#)

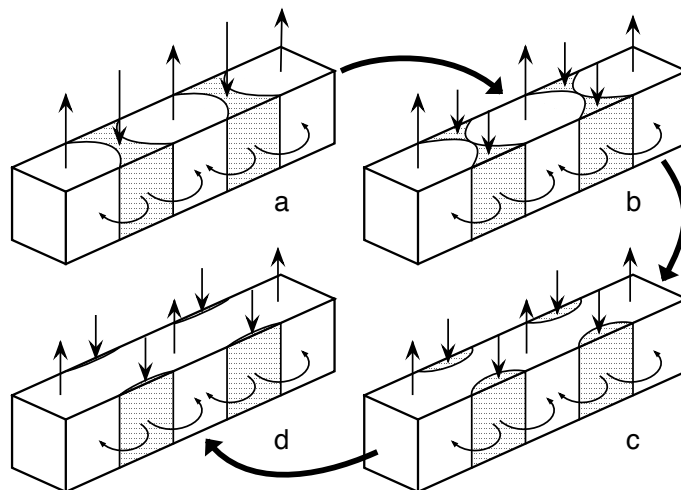


Figure 8. Stripe and channel domain configurations.

The origin of noise and magnetic hysteresis in permalloy fluxgate sensors

B. B. Narod

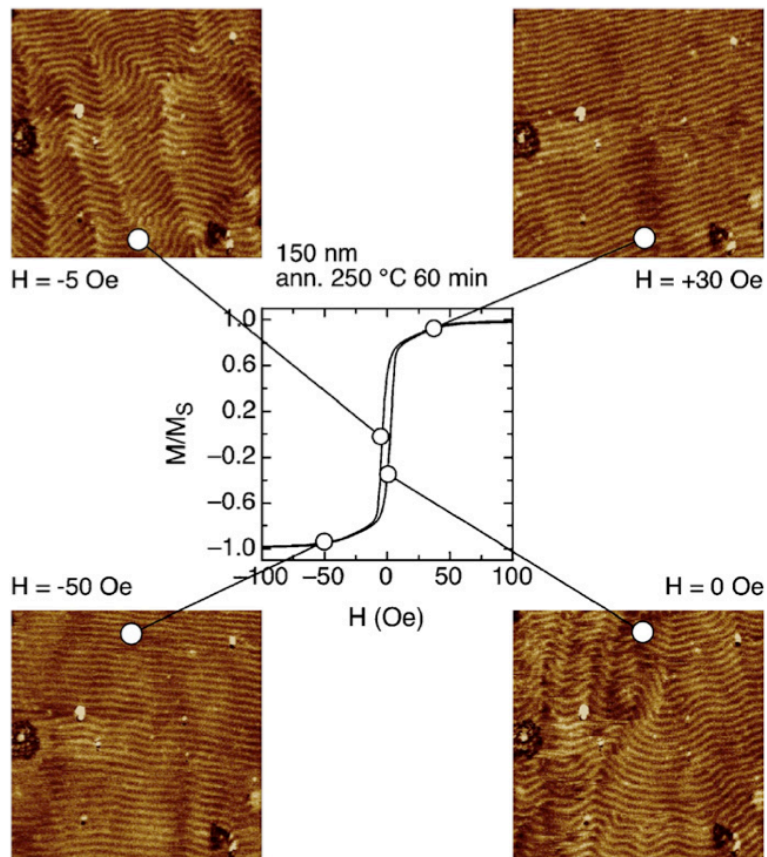


Figure 9. “Hysteresis loop of the 150 nm-thick film annealed at 250 °C for 60 min. Selected MFM images are shown, taken at different applied field values. The corresponding point of the hysteresis loop is indicated”. From Coïsson et al. (2009). (Non-SI units are in the original publication: $1 \text{ A m}^{-1} \cong 0.0126 \text{ Oe.}$) The specimen was a sputtered FeSiB amorphous film.

[Title Page](#)

[Abstract](#)

[Introduction](#)

[Conclusions](#)

[References](#)

[Tables](#)

[Figures](#)

[⏪](#)

[⏩](#)

[◀](#)

[▶](#)

[Back](#)

[Close](#)

[Full Screen / Esc](#)

[Printer-friendly Version](#)

[Interactive Discussion](#)

GID

4, 319–352, 2014

The origin of noise and magnetic hysteresis in permalloy fluxgate sensors

B. B. Narod

[Title Page](#)

[Abstract](#)

[Introduction](#)

[Conclusions](#)

[References](#)

[Tables](#)

[Figures](#)

[⏪](#)

[⏩](#)

[◀](#)

[▶](#)

[Back](#)

[Close](#)

[Full Screen / Esc](#)

[Printer-friendly Version](#)

[Interactive Discussion](#)

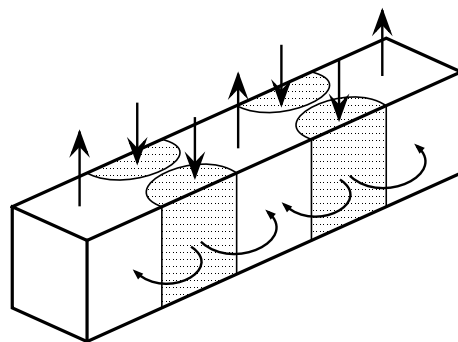


Figure 10. Expanding channel domains.

The origin of noise and magnetic hysteresis in permalloy fluxgate sensors

B. B. Narod

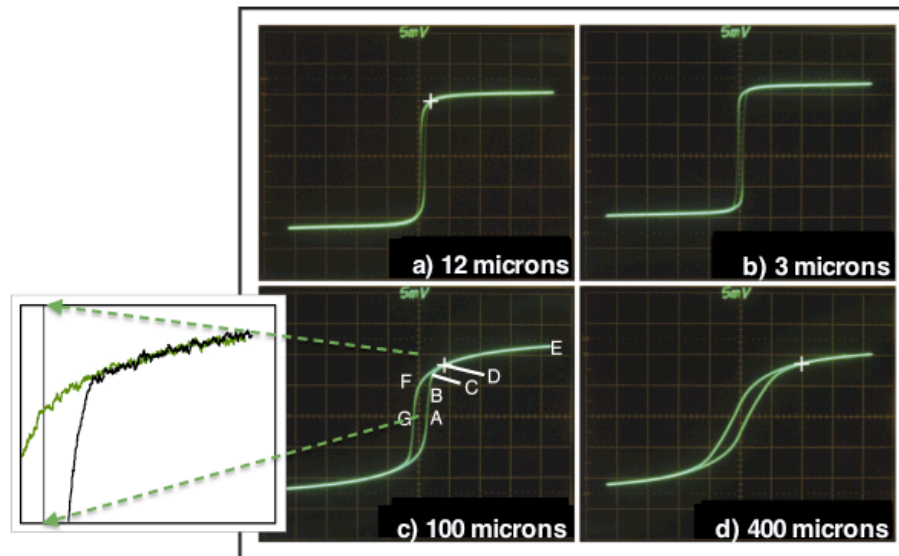


Figure 11. Infinetics 12 and $3\mu\text{m}$ B – H curves (top row). 6–81 $100\mu\text{m}$ and $400\mu\text{m}$ (bottom row). The drive field is $\pm 110\text{A m}^{-1}$, a triangle waveform at 25 Hz to approximate DC behaviour. The inset for (c) presents a digitally acquired detail of the distinct transition from irreversible behaviour to reversible behaviour. The argument presented here is that there are no Barkhausen jump related losses above the transition point, and that the large variation in B above the transition point requires reversible domain wall motion in the form of channel domain compression.

[Title Page](#)

[Abstract](#)

[Introduction](#)

[Conclusions](#)

[References](#)

[Tables](#)

[Figures](#)

[⏪](#)

[⏩](#)

[◀](#)

[▶](#)

[Back](#)

[Close](#)

[Full Screen / Esc](#)

[Printer-friendly Version](#)

[Interactive Discussion](#)

The origin of noise and magnetic hysteresis in permalloy fluxgate sensors

B. B. Narod

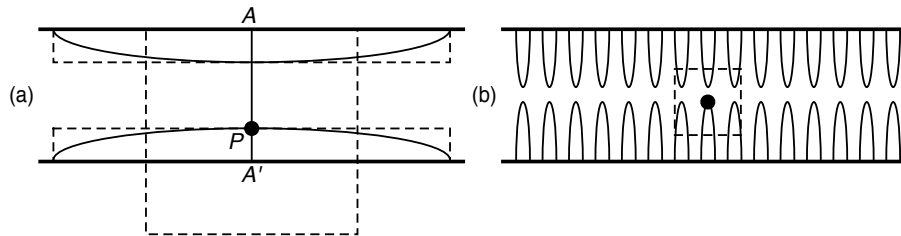


Figure 12. Channel domain sections: **(a)** thin foils, **(b)** thick foils.

[Title Page](#)

[Abstract](#)

[Introduction](#)

[Conclusions](#)

[References](#)

[Tables](#)

[Figures](#)

[◀](#)

[▶](#)

[◀](#)

[▶](#)

[Back](#)

[Close](#)

[Full Screen / Esc](#)

[Printer-friendly Version](#)

[Interactive Discussion](#)



The origin of noise and magnetic hysteresis in permalloy fluxgate sensors

B. B. Narod

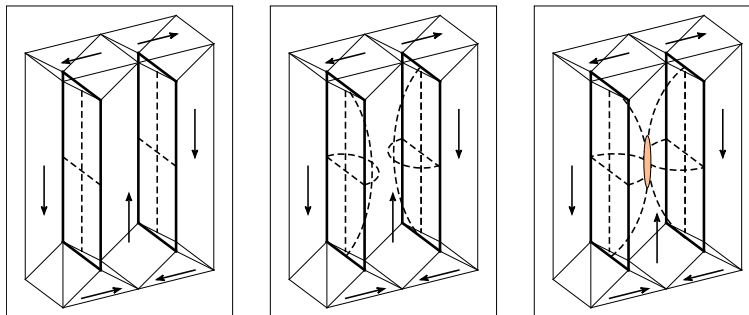


Figure 13. 3-dimensional representation of a single grain and stripe-to-channel reconnection. The left panel depicts the unmagnetized stripe domains within a grain. A larger grain would contain additional domains, all of the same width. The right panel depicts the start of reconnection at the domain wall midpoint. A fixed amount of domain wall displacement is required, regardless of the size of the grain. A larger grain would also have longer stripe domains and require less external field for a given amount of wall displacement, that is, higher initial permeability. Higher initial permeability in combination with a fixed amount of wall displacement for reconnection implies lower coercivity. Thus increasing grain size leads directly to higher permeability and lower coercivity.

[Title Page](#)

[Abstract](#)

[Introduction](#)

[Conclusions](#)

[References](#)

[Tables](#)

[Figures](#)

⏪

⏩

◀

▶

[Back](#)

[Close](#)

[Full Screen / Esc](#)

[Printer-friendly Version](#)

[Interactive Discussion](#)

The origin of noise and magnetic hysteresis in permalloy fluxgate sensors

B. B. Narod

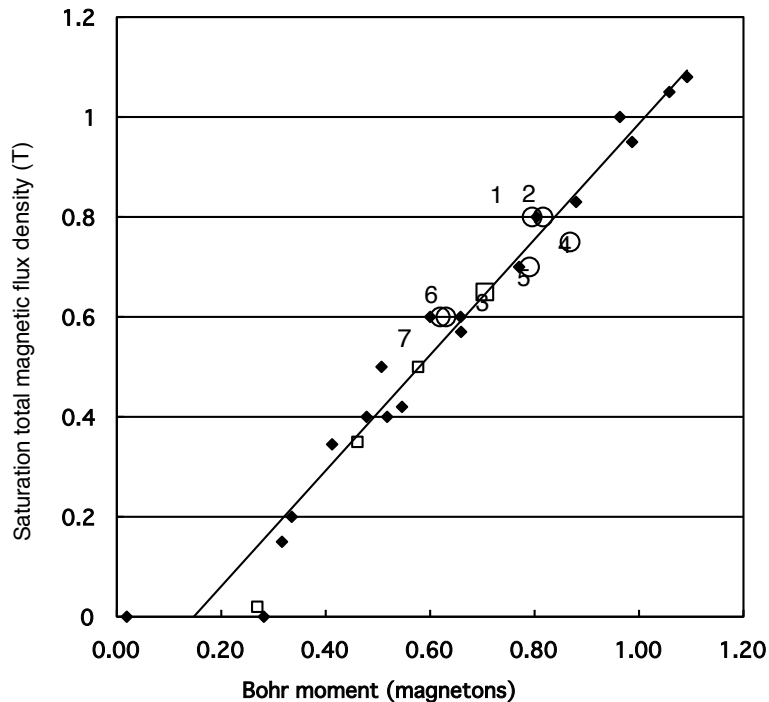


Figure 14. Saturation total magnetic flux density vs. average atomic moment. Data are from Neumann (1934), von Auwers and Neumann (1935), Bozorth (1951) or are calculated estimates. Large, open symbols plot alloys: (1) 14% Cu, (2) mumetal, (3) “6-81”, (4) 4-79, (5) supermalloy, (6) “1040”, (7) 28% Cu. Small symbols plot B_s data for a range of ternary alloys.

[Title Page](#)

[Abstract](#)

[Introduction](#)

[Conclusions](#)

[References](#)

[Tables](#)

[Figures](#)

[⏪](#)

[⏩](#)

[◀](#)

[▶](#)

[Back](#)

[Close](#)

[Full Screen / Esc](#)

[Printer-friendly Version](#)

[Interactive Discussion](#)